Unsaturated Flow Effects on Solute Transport in Soils

Luwen Zhuang[1, 2*], Amir Raoof[2], Mojtaba G. Mahmoodlu[2, 3], Sara Biekart[2], Riemer de Witte[2], Lubna Badi[2], Martinus Th. van Genuchten[2, 4], and Kairong Lin

[1]School of Civil Engineering, Sun Yat-sen University, Zhuhai, China

[2]Department of Earth Sciences, Utrecht University, P.O. Box 80021, 3508 TA, Utrecht, Netherlands

[3]Department of Watershed and Rangeland Management, Gonbad Kavous University, Iran

[4]Center for Environmental Studies, São Paulo State University, UNESP, Rio Claro, SP 13506-900, Brazil

*Corresponding author: Luwen Zhuang (luwen.zhuang@outlook.com)

Key points:

- Centimeter- and decimeter-scale column experiments were done to explore the effects of saturation and soil type on solute dispersivity.
- A clear non-monotonic relationship was found between the dispersivity and soil water saturation.
- The extent of non-monotonicity was more pronounced for relatively coarse-textured soils, but less for finer soils.

Abstract

A major transport process in soils is hydrodynamic dispersion which affects the spreading and arrival of surface-applied pollutants at underlying groundwater reservoirs. When a soil is unsaturated, hydrodynamic dispersion is very much affected by soil water saturation. Centimeter-scale and decimeter-scale column experiments were carried out to explore the effects of fluid saturation and soil type on the unsaturated soil solute dispersivity. Measured in-situ breakthrough curves were analyzed in terms of both classical advection-dispersion and dual-porosity (mobile-immobile) type transport equations. A clear non-monotonic relationship was found between the dispersivity and soil water saturation. The extent of non-monotonicity was more pronounced for relatively coarse-textured soils compared to the finer soils. This finding has been reported rarely before; it explains the inconsistency of saturation-dispersivity relationships in the literature. The relationship between solute dispersivity and water saturation proposed herein may improve the performance of field-scale transport models for the unsaturated zone.

Keywords: dispersion, dispersivity, solute transport, unsaturated zone

1. Introduction

Contaminants released at or near the earth surface may travel through the soil unsaturated zone to arrive at and pollute underlying groundwater resources. Knowledge of the processes governing the fate and transport in the unsaturated zone is a major aspect of risk assessments and remediation of contaminated aquifers (Bear & Cheng, 2010). Many studies have been carried out to investigate solute transport processes in the saturated zone (e.g., Fitch & Jia, 1996; Chiogna et al., 2010; Rolle et al., 2010; Gai et al., 2011). Soil texture and travel distance are well-known for influence the dispersion significantly. An additional complexity in the unsaturated (vadose) zone is the effect of soil water content (or fluid saturation) on solute dispersion (Bear, 1988), an issue that remains relatively ill-defined (Scheidegger, 1961; Yule & Gardner, 1978; Bolt, 1979; De Smedt et al., 1986; Gelhar, 1986). Several studies (e.g., Kirda et al., 1973; De Smedt et al., 1986; Maraqa et al., 1997; Matsubayashi et al., 1997; Devkota et al., 1998; Padilla et al., 1999; Kumahor et al., 2015) have shown an increase in the solute dispersivity for unsaturated soils compared to fully saturated conditions, while others(e.g., Vanderborght & Vereecken, 2007) reported a decrease with desaturation. Still other studies (Yule & Gardner, 1978; Costa & Prunty, 2006) found that dispersion remains constant, regardless of desaturation. A few recent experimental studies (Bunsri et al., 2008; Toride et al., 2003; Karadimitriou et al., 2016) have shown a non-monotonic relationship between the solute dispersivity and soil water content, with the dispersivity increasing to a maximum value (referred to here as the critical dispersivity) at some intermediate saturation and then decreasing with further desaturation. Raoof and Hassanizadeh (2013) could explain this non-monotonic dispersivity behavior based on a numerical study of pore-scale fluid flow and solute transport processes.

The discrepancies in the literature referred to above are likely due in part to different soil types being used in the various studies. Soil texture and soil structure affect water and air distributions at a given saturation, which in turn affects prevailing fluid velocity variations and should lead to different solute spreading and dispersion phenomena. Additionally, scale effects are important for solute dispersion (e.g., Dagan, 1986; Butters et al., 1989; Bromly & Hinz, 2004; Bromly et al., 2007; Mayer et al., 2008); however their impact under unsaturated conditions are not clear.

Another unsettled issue is the selection of an appropriate macro-scale model, which could be the classical equilibrium Advection-Dispersion Equation (ADE), a dual-porosity type Mobile-

Immobile Model (MIM), or some other formulations. Some studies suggested the use of MIM type models (e.g., De Smet et al., 1981; Beven & Young, 1988; Geiger & Durnford, 2000) while others (e.g., Maraqa et al., 1997) show the suitability of the ADE to model transport without requiring immobile liquid zones. Still, the various transport models do need relationships for macroscopic coefficients related to solute dispersion and possible nonequilibrium mass transfer processes. Similar to the constitutive relationships for fluid flow, transport parameters are known to depend on pore structure as well as on actual air and water phase distributions. Lack of available constitutive data is often cited as a primary barrier to acceptable predictions (Toride et al., 2003).

Although advection and dispersion are generally considered to be the most important transport processes, there is ample evidence that solute diffusion into immobile or dead-end zones contributes to increased solute residence times. In addition, vapor transport within air-filled pores can significantly enhance the migration of contaminants from their sources if volatile contaminants are involved (Raoof & Hassanizadeh, 2013). Criteria are needed for choosing a particular macro-scale model that can be used for different soil types and fluid saturation scenarios, including variably-saturated conditions. Unfortunately, only a few well-controlled laboratory-scale hydrodynamic dispersion experiments exist for unsaturated flow conditions, especially experiments that consider a broad range of saturations. One major reason for this relates difficulties to establish uniform flow conditions at relatively low fluid saturations.

In this paper we present results of a complete and systematic numerical and experimental study on solute transport under saturated and unsaturated conditions. Our aim is to investigate several factors influencing unsaturated transport, such as soil texture and scale effects. We performed a series of solute transport experiments for different sandy soils with a wide range of fluid saturations. Moreover, we employed two experimental setups with different column lengths to explore the scale dependency of unsaturated solute dispersion. Breakthrough curves (BTCs) were measured in situ at different points along the flow path. The equilibrium ADE and nonequilibrium-based MIM models were used to analyze the experimental data and to obtain solute dispersivities at different saturations. The resulting dependency of the solute dispersivity on water saturation is shown and discussed.

2. Materials and Methods

2.1. Materials

Two different sands were used in the experiments. A relatively fine sand, S1, was obtained from a mining site in Belgium, and a coarse sand, S2, from a riverbed in the Netherlands. Before their use we washed the sands using deionized water to remove clay particles. Properties of the two sands are listed in Table 1. The HYPROP evaporation device (UMS AG, Germany) was used to measure soil water retention data of the two sands, and to find the corresponding van Genuchten (1980) soil hydraulic parameters. The resulting curves are shown in Figure 1, while the optimized hydraulic parameter values are listed in Table 1. Compared with sand S1, sand S2 had a lower air entry pressure as reflected by a larger α value, and a larger residual water saturation value.

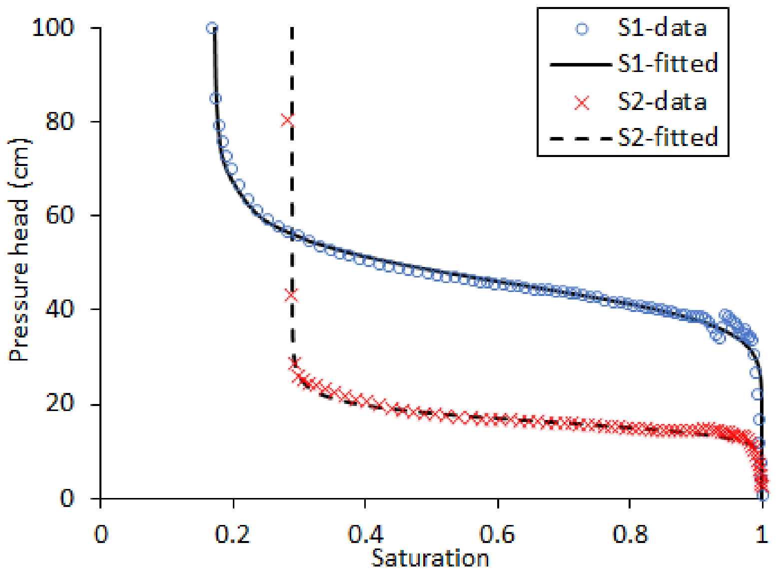

Figure 1. Water retention data for fine sand S1 and coarse sand S2

Table 1. Properties of sands S1 and S2 used in the experiments

Properties	S1	S2
Particle size (mm)	0.1-0.5	0.3-0.8
Mean particle diameter, d_{50} (mm)	0.20	0.50
Uniformity coefficient, d_{60}/d_{10}	1.7	1.2
van Genuchten parameter, α (cm^{-1})	0.022	0.062
van Genuchten parameter, n (-)	10.0	10.0
Irreducible water saturation, S_r (-)	0.17	0.29
Saturated conductivity, K_s (cm min^{-1})	1.02	4.80
Average porosity, φ (-)	0.39	0.37

2.2. Experimental Apparatus and Procedures

We employed a 37-cm long plexiglass column with an inner diameter of 10 cm to perform the unsaturated flow and solute transport experiments. The setup is shown in Figure 2. Since the dispersivity is sensitive to possible nonuniformities of flow across the inlet boundary, we placed a very permeable porous plate at the top of the column to uniformly distribute water over the entire inlet surface area. A 5-mm thick hydrophilic filter was used at the bottom of the column to serve as a capillary barrier preventing air penetration into the sample. A vacuum pump furthermore was used at the outlet to precisely control the outlet water pressure head.

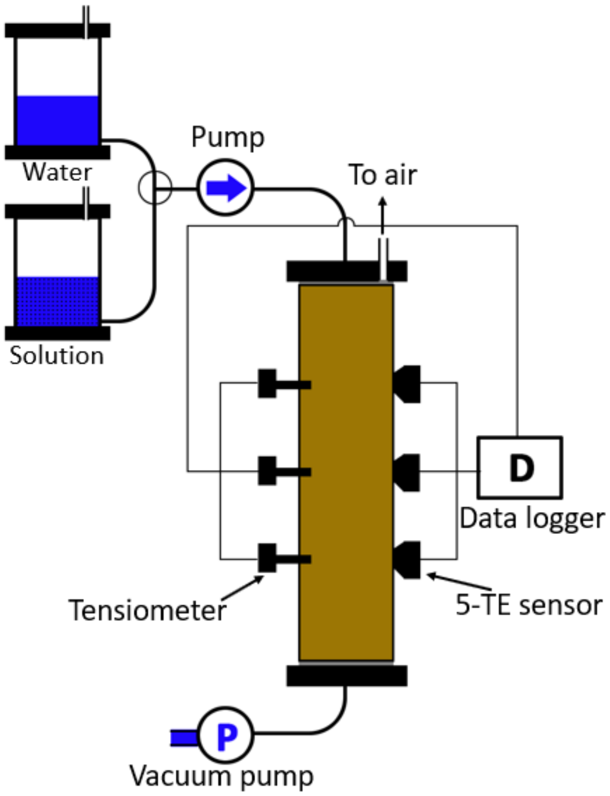

Figure 2. Schematic view of the 37-cm long column

The columns were packed by pouring dry sand into the water-filled columns. During packing, we regularly tapped the sands and scratched their surface to avoid layering. Deionized and degassed water was used in all experiments. Several sensors were used for the required measurements. Three micro-tensiometers (Rhizo Instruments, Netherlands) were installed at depths of 10.5, 18.0, and 25.5 cm, respectively, to measure pressure heads along the samples. The tensiometers consisted of a ceramic cup having dimensions of 1 cm in length and 4 mm in diameter, as well as a small pressure transducer. We further inserted probes (5-TE sensors, Decagon Devices, USA) at the same depths to obtain the electrical conductivity at those locations. This allowed us to also estimate water saturation of a given sample from the electrical conductivity using the Topp empirical formula (Topp et al., 1980). When injecting a tracer solution, the solute concentration is linearly related to the electrical conductivity at a given value of water saturation (Toride et al., 2003). All data were collected using a CR1000 data logger (Campbell Scientific, UK).

Solute transport experiments were carried out under both saturated and unsaturated flow conditions. The saturated flow experiments involved two different flow rates. After establishing steady-state flow using pure water, a three-way valve was used to start injecting a $CaCl_2$ solution (0.08 mol/L) for a certain pore volume, and then returning to pure water to create a solute pulse. Concentration breakthrough curves (BTCs) were measured at three depths using the 5-TE sensors. For the transport experiments during unsaturated flow, unit-gradient flow was established before injecting the solute pulse at a given water saturation. This was done to obtain uniform water contents (i.e., no gradients in the capillary pressure) in the samples, which later allowed us to relate the observed solute dispersivity to a certain well-defined saturation value. To do so, starting from saturated flow conditions, the water inflow rate at the top and water pressure head at the bottom of the column were decreased gradually in order to minimize local hysteresis effects. The top of the column was open to air to keep the air pressure fixed at the atmospheric level. During this process, we monitored the three tensiometers until they reached the same negative unsaturated water pressure head, thus ensuring that unit gradient flow was achieved.

The solute dispersivity is known to be length-scale dependent. To investigate this effect at the laboratory scale, we performed, in addition to the experiments using 37-cm long sand columns, also transport experiments using a much smaller sample. The smaller sample had dimensions of 3 cm (height) by 3 cm (length) by 2 cm (width), filled with S1 sand. A schematic view of the small sandbox system is shown in Figure 3. More details about the sample container can be found in Zhuang et al. (2017). For the smaller sample we used gamma ray transmission to measure water saturations and solute concentrations, thus avoiding the insertion of any physical sensors into the small sample. This would avoid any disturbance of the soil by sensors, including possible gaps between the surface of the sensors and the soil particles. Measurement of the attenuation of gamma photons has been often used to determine the soil bulk density and water content, but not solute concentrations. For this study, we calibrated the attenuation to be able to also measure solute concentrations. Detailed information about the gamma transmission method is given in the Supporting Information Text S1.

The transport experiments in the sandbox under saturated flow conditions were carried out using two different water flow rates. For unsaturated flow conditions, a continuous flux was applied to the sand sample in the sandbox starting from primary drainage. After packing the saturated sand samples, we applied a flow rate slightly smaller than the measured saturated hydraulic conductivity (obtained with the constant-head method) to the top of the sample. The hanging water column was then kept at the same level as the bottom of the sand sample. Readings of the two tensiometers were monitored continuously. When readings of two tensiometers were identical, water saturation of the sample was measured using the gamma system. The three-way valve subsequently was switched from solute-free water to a $CaCl_2$ solution for a certain pore volume, and then switched back to solute-freewater in order to create a solute pulse. The residual concentration breakthrough curves (BTCs) were measured every 30 s using the gamma system.

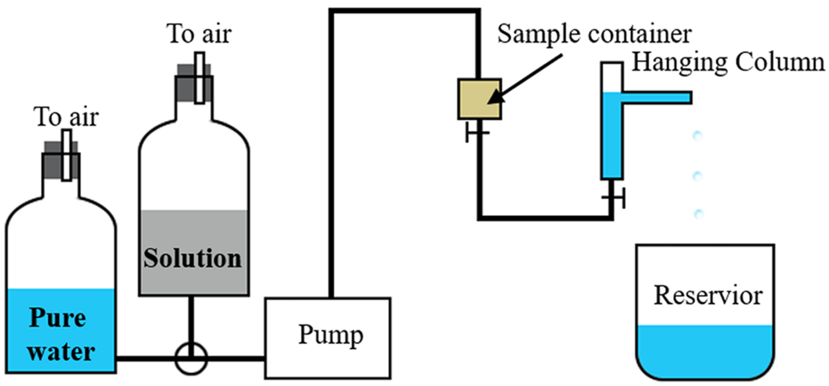

Figure 3. Schematic view of the 3-cm long sandbox system

In all we conducted eight experiments for sand S1 and ten experiments for sand S2 using the long column under variably-saturated flow conditions. The BTCs were observed at three depths for each experiment. For the small sample, we carried out eight experiments for sand S1 under both saturated and unsaturated flow conditions. The BTCs in the small column were measured at 1.5 cm from the inlet, with each experiment carried out twice at least to validate the results.

2.3. Transport Models

Since solutes were injected uniformly across the entire inlet cross section, and the lateral boundaries were no-flow, overall macroscopic flow and solute transport in both setups can be considered to be one dimensional. The BTCs hence could be simulated using one-dimensional continuum scale modeling. Two different formulations were considered for this purpose: The Advection Dispersion Equation (ADE) and a dual-porosity type Mobile-Immobile model (MIM). We used the STANMOD software (Toride et al., 1995; Šimůnek et al., 1999) for all forward and inverse calculations.

For non-reactive solute transport such as in this study, the ADE is given by

$$\frac{\partial C}{\partial t} = D\frac{\partial^2 C}{\partial x^2} - v\frac{\partial C}{\partial x} \tag{1}$$

where C represents the solute concentration, v denotes the pore velocity, D is the hydrodynamic longitudinal dispersion coefficient, t is time, and x is the spatial coordinate. The dispersivity λ in the ADE formulation is defined as $\lambda=D/v$, thus implying that diffusion in our study has negligible effect on longitudinal transport.

Nonequilibrium transport often exists during both saturated and unsaturated flow, leading to early arrival and tailing in observed BTCs (van Genuchten et al., 1977; De Smedt et al., 1986). One approach to account for this is to modify the ADE model to assume the presence of stagnant water in relatively small or dead-end pore spaces. MIM models consider total water saturation (S) to be made up of two regions: mobile water saturation (S_m) and immobile water saturation (S_{im}), with solute exchange between the two regions simulated as a first-order mass transfer process. The MIM model for non-reactive transport can be described as (Coats & Smith, 1964; van Genuchten et al., 1977)

$$S_m\frac{\partial C_m}{\partial t} + S_{im}\frac{\partial C_{im}}{\partial t} = S_m D_m\frac{\partial^2 C_m}{\partial x^2} - S_m v_m\frac{\partial^2 C_m}{\partial x} \tag{2}$$

$$\varphi S_{im}\frac{\partial C_{im}}{\partial x} = \omega\left(C_m - C_{im}\right) \tag{3}$$

where the subscripts m and im refer to the mobile and immobile regions, respectively, φ is the porosity, and ω is the mass transfer coefficient between the mobile and immobile regions. We will use the parameter β for the fraction between mobile to total saturation, i.e., S_m/S. The hydrodynamic dispersion coefficient for the mobile phase is represented by D_m, which is approximately equal to D/β. Similarly, the pore velocity v is equal to βv_m. The dispersivity λ_m in the MIM model is defined as $\lambda_m=D_m/v_m$.

We specified third-type inlet boundary conditions for both models, thus considering all concentration data to be volume-average variables (van Genuchten & Parker, 1984; van Genuchten & Wierenga, 1986). The dispersion coefficient D and the pore velocity v were the optimized parameters in the ADE model, while for the MIM model we also needed to optimize simultaneous the mass transfer coefficient ω and the mobile fluid ratio β.

3. Results and Discussion

3.1. Breakthrough Curves

First, we present a selection of the BTCs that were measured at different locations and for fluid saturations, and their analysis in terms of the ADE and MIM models. Fitted values of the transport parameters are listed in Tables S1 to S12 of the Supporting Information. We note here that application of different macroscopic models (ADE and MIM in our case) will lead to different parameter values depending upon the formulation of the macroscopic equations.

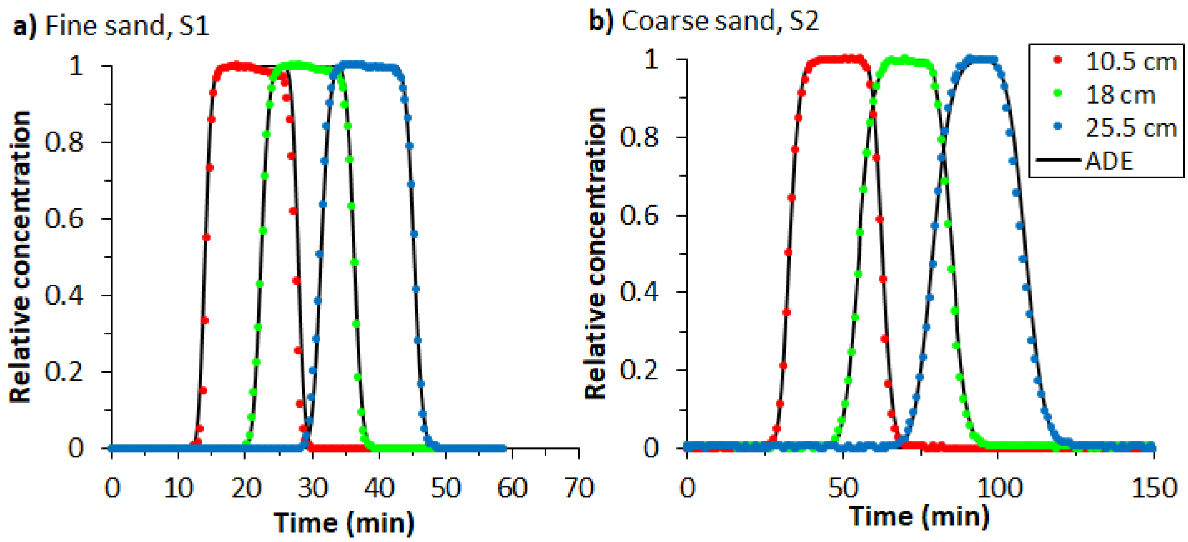

Figure 4. Saturated flow conditions: Observed and simulated BTCs for fine sand S1 and coarse sand S2.

Figure 4 shows BTCs obtained under saturated flow conditions. Both fine sand S1 and coarse sand S2 provided symmetrical BTCs at all depths. Given the symmetry, the ADE model was sufficient to describe the data (the black solid lines in Figure 4). By comparison, observed BTCs at intermediate saturation values, such as shown in Figure 5 for S=0.44, were less symmetrical with some tailing at both the higher and lower concentrations (van Genuchten et al., 1977; De Smedt et al., 1986). This suggests the use of the MIM model in addition to the

ADE. The results are shown in Figure 5 as solid and dash lines, respectively. The MIM model gave better agreement with the non-symmetric structure and tailing of the BTCs (R^2 values can be found in Tables S1-S12).

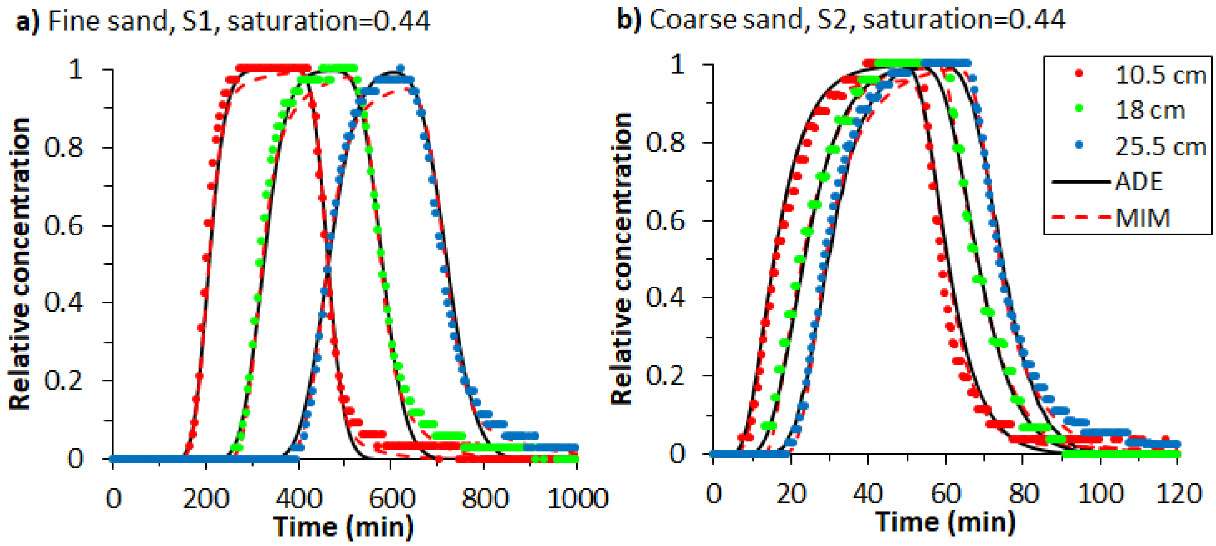

Figure 5. Unsaturated flow conditions: Observed and simulated BTCs, at S=0.44, for fine sand S1 and coarse sand S2.

3.2. Dispersivity in Different Models

3.2.1. ADE Model

Figure 6 shows estimated dispersivity values as a function of water saturation using the ADE model. The results clearly indicate non-uniform relationships between the solute dispersivity, λ, and saturation, S. The relatively fine sand (S1) column showed an increase in dispersivity as saturation decreased from 1.0 to 0.5, but then λ slightly decreased S became less than 0.5. This behavior is consistent for all depths. Overall, λ showed a slight non-monotonic behavior with a maximum value (i.e., the critical dispersivity) at an intermediate saturation value of 0.5. We note that only one set of the BTCs was measured for saturations less than 0.5 in sand S1. This because of the very low permeability of the fine sand at low saturations, and hence the extremely long times needed to obtain complete BTCs. Coarse sand S2 showed much more visible non-monotonic behavior and the associated critical dispersivity (Figure 6b). These results confirm that non-monotonicity exist in the dispersivity versus saturation, with the extent of non-monotonicity depending upon soil type (becoming less pronounced for finer sands). Moreover, the S value corresponding to the critical dispersivity shifted to a relatively large value of around 0.6 for coarse sand. Our results indicate that change in λ with fluid desaturation depends upon soil type, thus explaining some of the discrepancies about the unsaturated soil solute dispersivity reported in the literature. For instance, Toride et al. (2003) and Bunsri et al. (2008) showed non-monotonic relationships between λ and fluid saturation for 0.25-0.50 mm and 0.15-0.5 mm sand particle sizes, which are slightly coarser than our sand S1. By comparison, Padilla et al. (1999) reported a monotonic dispersivity-saturation relationship for their sand ranging from 0.2-0.5 mm (finer than our sand S1).

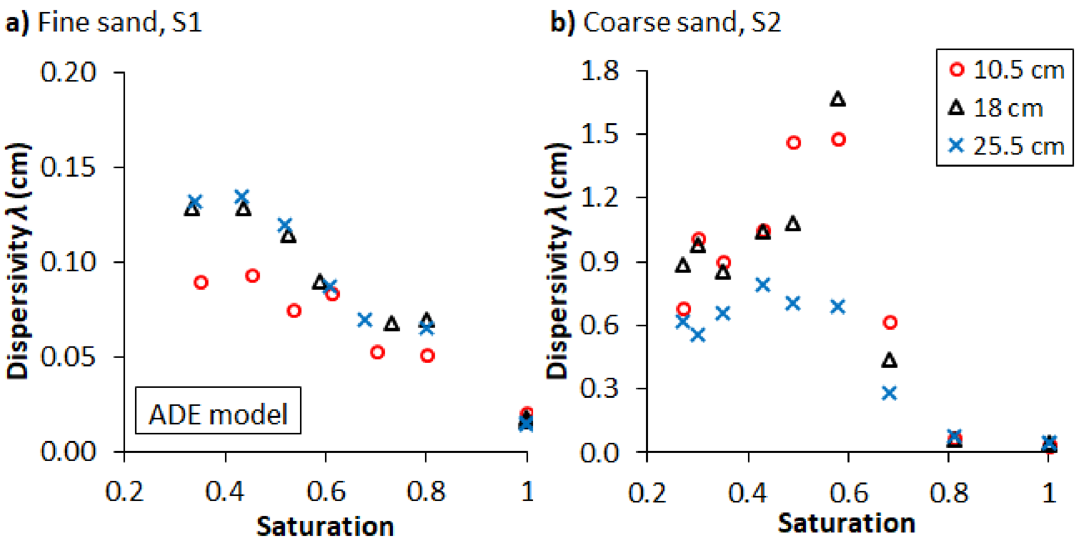

Figure 6. ADE model results: dispersivity, λ, versus water saturation at different depths for fine sand, S1 (a), and coarse sand, S2 (b).

At a given saturation level, the dispersivity changes with distance due to its scale dependency. Our results showed an increase in the dispersivity up to a distance of 18.0 cm, where it reached to an asymptotic value for sand S1. The finer sand, S2, was found to be less sensitive to the length scale. To further explore this effect, we used a non-destructive method (to prevent sample disturbance) to collect dispersivity data for the fine sand, S1.

3.2.2. MIM Model

Changes in the dispersivity obtained with the MIM model (i.e., the mobile phase dispersivity, λ_m) as a function of water saturation for both sands are shown in Figure 7a. The transport parameters were obtained using the BTCs at the central location (i.e., at 18.0 cm) since they are affected here the least by the inlet and outlet boundaries.

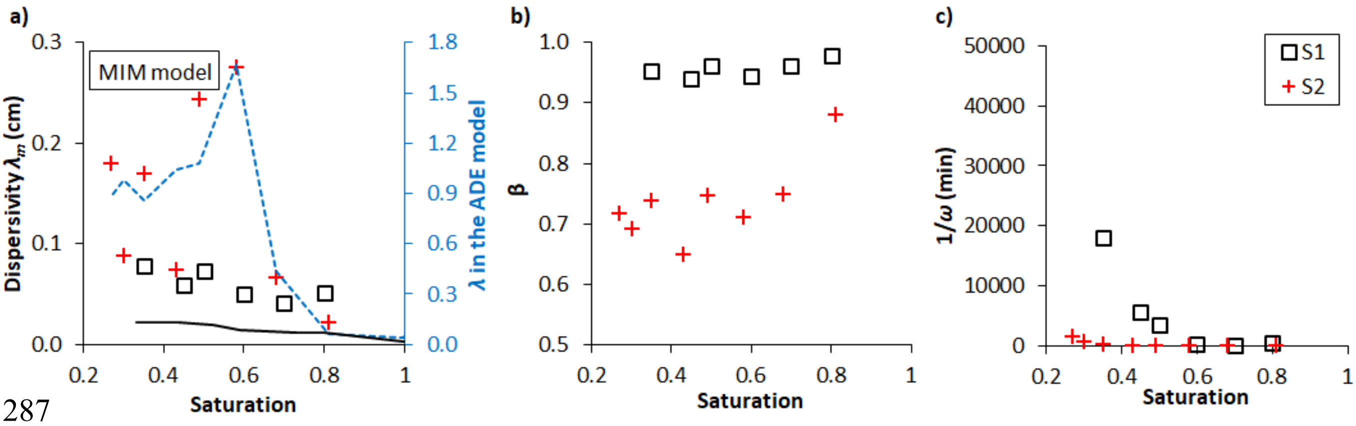

Figure 7. Changes in solute transport parameters with saturation using the MIM model: variations in a) solute dispersivity of the mobile phase, λ_m, b) the mobile phase fraction, $\beta=S_m/S$, and c) the mass transfer equivalent time between the mobile and immobile phases, $1/\omega$. For comparison, the corresponding λ values using the ADE are shown as lines.

Dispersivity values obtained with the MIM model were smaller than those obtained using the ADE over the entire saturation range. This can be explained by the fact that solute mixing in the MIM is represented using two parameters (i.e., the dispersivity and the mass transfer coefficient) while in the ADE all of the mixing processes are lumped into a single dispersivity parameter. The relationship between λ_m and water saturation for coarse sand S2 showed a non-monotonic relation, similar as for the ADE model. However, the values of λ_m were six times smaller than the λ values.

Mass exchange between the mobile and immobile liquid phases is influenced by the relative amount of these phases and the mass transfer coefficient associated with this exchange. Figure 7b presents the ratio (β) between mobile water saturation (S_m) and total saturation (S). The mobile water fraction was at its maximum during saturated conditions, but decreased as more air occupied the soil pores at lower saturation values. For fine sand S1, β values decreased slightly and then remained nearly constant at a value of 0.96 as S further decreased. For coarse sand S2, β values decreased significantly at first, but then stayed at around 0.7 with further desaturation. Differences in the pore sizes between the two sands are the main cause of the differences in β. Sand S1 is a relatively fine to medium sand with relatively small pores, while sand S2 is a coarse sand with much larger pores. During primary drainage, water in the larger pores drain fast at first, with some parts of water in the larger pores becoming isolated and immobile, whereas water in the smaller pores becomes disconnected more gradually as saturation decreases. Therefore, for sand S2, drainage of the larger pores created considerably more immobile water.

Figure 7c shows the mass transfer equivalent time, $1/\omega$, as a function of saturation under unsaturated flow conditions. For fine sand S1, when $S>0.6$, the transfer time was very small, implying rapid solute exchange, while the transfer time increased dramatically by two orders of magnitude or more when $S<0.6$. For coarse sand S2, the transfer time was very small over the entire saturation range, with a slight increase only when $S<0.3$. Mass transfer hence required far less time for coarser sand S2 compared to finer sand S1.

3.3. Dispersivity at Different Scales

The above experiments were carried out using 37-cm long columns. We additionally used a very short 3-cm column to perform transport experiments for the fine sand, S1. The resulting parameter values for the short column are listed in Table S13. Selected BTCs under saturated and unsaturated flow conditions are shown in Figure 8. The BTCs exhibited some scattering in the concentration values, most likely due to local flow variations (the measurement area normal to the of ray flux was only 6 mm in diameter) and subsequent dynamic changes in the air-water interfaces during gamma ray passage. We acknowledge here that BTCs from very short columns inherently are affected more by experimental imperfections associated with packing and the implementation of boundary conditions.

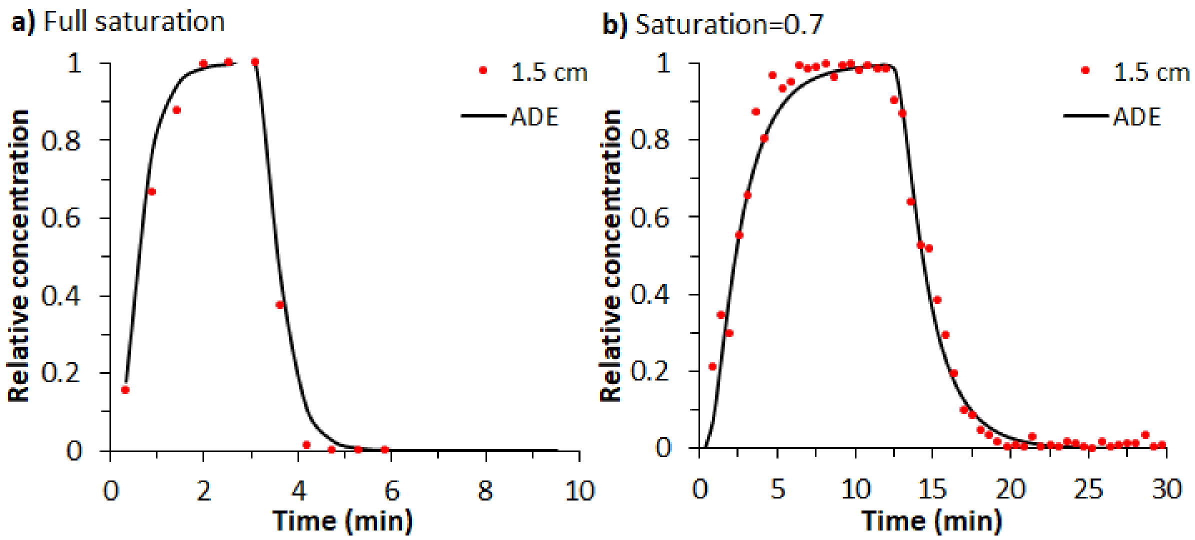

Figure 8. Saturated and unsaturated flow conditions: Observed and simulated BTCs for fine sand S1 using the 3-cm sample.

Figure 9a shows a plot of normalized dispersivity values (relative to saturated λ values) obtained using both the small, 3-cm, sample as well as the larger, 37-cm, columns. The inset provides a view with a smaller scale of the *y* axis. As saturation decreased, λ values obtained with the small sample for fine sand S1 increased to around 0.6 cm at S=0.5, and then decreased slightly (i.e., again showing a non-monotonic relationship). By comparison, the dispersivities obtained for coarse sand S2 were much more non-monotonic. Still, all of the samples with their different soil types and sample lengths confirmed a saturation dependency of the solute dispersivity, with the dependency being far more pronounced and non-monotonic for the coarser sand (Figure 9a). For the finer sand, for which we performed experiments with two different sample lengths, saturation had much more effect on the dispersivity of the longer column, but with the non-monotonicity being far less as compared to the coarser sand. Fluid saturation at the turning point (the critical saturation S_c) was slightly lower for fine sand S1 (S_c=0.5) compared to the coarse sand S2 (S_c=0.6).

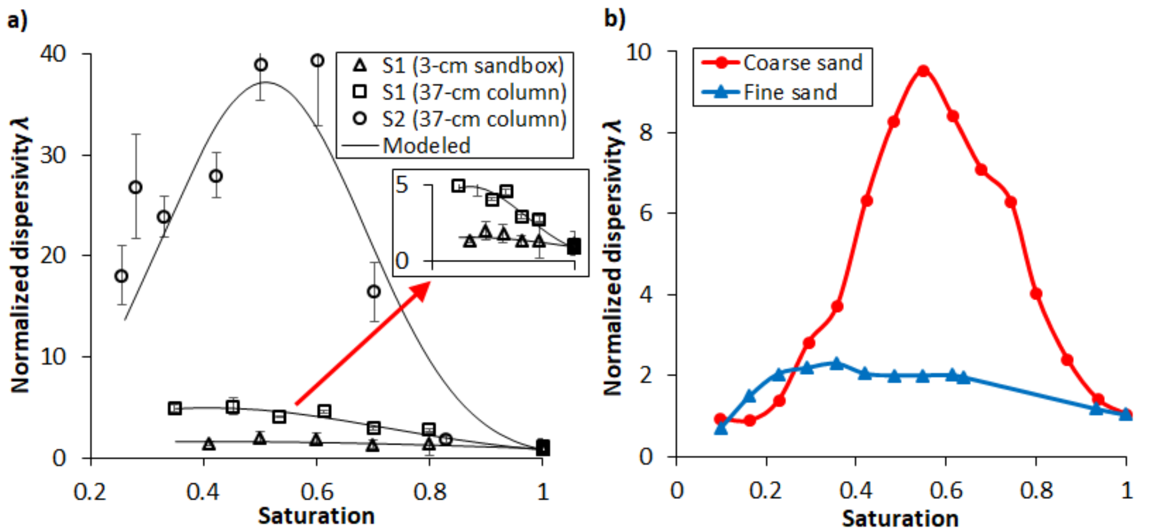

Figure 9. a) Comparison of normalized dispersivity values, λ, using the ADE model for both sands, as well as for different sample sizes for sand S1, and b) relationships between the normalized dispersivity λ and saturation reported in the literature (Raoof & Hassanizadeh, 2013) based on 3D pore scale modeling of samples with different pore sizes, showing a monotonic behavior. Values of λ in a) for the larger columns were for the BTCs at 10.5 cm (closest to the inlet of the columns); solid lines show the fitted relationships to the data.

Interestingly, the results in Figure 9a show a similar trend as found in previous studies where 3D pore-scale modeling was used to explore the saturation dependency of the dispersivity using samples with different pore size distributions (Figure 9b, Raoof & Hassanizadeh, 2013). Consistent with that study, the experimental observations can be explained by the underlying pore scale processes. For unsaturated conditions, λ is affected by the amount of mixing at the level of individual pores, which becomes limited due to the presence of air in the larger pores. Furthermore, at the level of sample size, dispersivity is affected by pore connectivities and whether in an unsaturated soil a cluster of connected saturated pores exist to form a flow pathway that percolates though the entire sample. Sample S2 has larger pores and a wider distribution of pore sizes as reflected also by its capillary pressure-saturation curve and the higher saturated dispersivity values. In this sample, air during drainage enters larger pores and effectively disconnects them from the otherwise connected saturated pore system that forms fast flow pathways through the soil. Eliminating these pathways causes velocity variations to become less among different parts of the sample and, therefore, causes λ to decrease. Raoof and Hassanizadeh (2013) showed that this dispersivity turning point (λ_c) occurs at higher saturation values for soils having larger pore sizes, consistent with our observations (Figure 9).

For a soil with smaller pore sizes (e.g., sand S1) the effect of pathways and their elimination by the invading air phase become less distinct which is also supported by pore scale studies. For such a sample, the turning point of the dispersivity occurs at lower saturations, while changes in λ are affected less by saturation compared with samples having larger pore sizes.

To describe the relationship between the dispersivity and saturation explicitly, we propose an empirical formula with a Gaussian shape as follows

$$\lambda(S) = ae^{-\left(\frac{S-b}{c}\right)^2} \tag{4}$$

in which a, b, and c are fitting parameters. We applied Equation (4) to the three sets of λ-S data. The resulting curves are shown as solid lines in Figure 9a, while the parameter values are given in Table 2. The values of a and b were close to the maximum dispersivity and the critical saturation, respectively. Knowing the maximum dispersivity and the critical saturation, it is then possible to predict λ over the entire saturation range (especially saturation levels larger than residual saturation). Equation (4) could be used for field-scale modeling of solute transport in the unsaturated zone.

Table 2. Values of the parameters in Equation (4) for sands S1 and S2

Experiment	a	b	c
S1-sandbox	1.50	0.41	0.81
S1-column	4.91	0.45	0.39
S2-column	37.2	0.49	0.24

4. Conclusions

This study provides a comprehensive analysis of solute transport for different sandy soils under saturated and a wide range of unsaturated flow conditions. Results showed a well-defined dependence of the solute dispersivity on soil water saturation, with the resulting relationship being non-monotonic, particularly for the coarser medium.

The established relationship between solute dispersivity and water saturation may prove to be important for field-scale models of the unsaturated zone to provide a better basis for subsurface environmental management and risk analyses. Our study involved carefully packed homogeneous fine and coarse sands. Further studies are needed for different natural soils, especially structured or macroporous field soils, to identify or improve possible relationships between the solute dispersivity and water content in the unsaturated zone.

Acknowledgments

The authors acknowledge the financial support by the Veni Talent Scheme Award (No. 016.151.047), which is (partly) financed by the Netherlands Organization for Scientific Research (NWO), and the outstanding Youth Science Foundation of NSFC (No. 51822908). The data from this work are available at https://doi.org/10.6084/m9.figshare.11689233.v3.

References

Bear, J. (1988). *Dynamics of fluids in porous media*. *Dover*. https://doi.org/10.1097/00010694-197508000-00022

Bear, J., & Cheng, A. H.-D. (2010). *Modeling groundwater flow and contaminant transport*. *Springer*. https://doi.org/10.1017/CBO9781107415324.004

Beven, K. J., & Young, P. C. (1988). An Aggregrated mixing zone model of solute transport through porous media. *Journal of Contaminant Hydrology*, *3*, 129–143. https://doi.org/http://dx.doi.org/10.1016/0169-7722(88)90028-9

Bolt, G. H. (1979). Movement of solutes in soil: Principles of adsorption/exchange chromatography. In G. H. B. T.-D. in S. S. Bolt (Ed.), *Soil Chemistry: B. Physico-Chemical Models,Dev.Soil Sci.* (Vol. 5B, pp. 295–348). Elsevier. https://doi.org/https://doi.org/10.1016/S0166-2481(08)70664-0

Bromly, M., Hinz, C., & Aylmore, L. A. G. (2007). Relation of dispersivity to properties of homogeneous saturated repacked soil columns. *European Journal of Soil Science*, *58*, 293–301. https://doi.org/10.1111/j.1365-2389.2006.00839.x

Bromly, M., & Hinz, C. (2004). Non-Fickian transport in homogeneous unsaturated repacked sand. *Water Resources Research*, *40*, W07402. https://doi.org/10.1029/2003WR002579

Bunsri, T., Sivakumar, M., & Hagare, D. (2008). Influence of dispersion on transport of tracer through unsaturated porous media. *Journal of Applied Fluid Mechanics*, *1*(2), 37–44.

Butters, G. L., Jury, W. A., & Ernst, F. F. (1989). Field scale transport of bromide in an unsaturated soil: 1. Experimental methodology and results. *Water Resources Research*, *25*(7), 1575–1581. https://doi.org/10.1029/WR025i007p01575

Chiogna, G., Eberhardt, C., Grathwohl, P., Cirpka, O. A., & Rolle, M. (2010). Evidence of compound-dependent hydrodynamic and mechanical transverse dispersion by multitracer laboratory experiments. *Environmental Science and Technology*, *44*(2), 688–693. https://doi.org/10.1021/es9023964

Coats, K. H., & Smith, B. D. (1964). Dead-end pore volume and dispersion in Porous Media. *Society of Petroleum Engineers Journal*, *4*(01), 73–84. https://doi.org/10.2118/647-pa

Costa, J. L., & Prunty, L. (2006). Solute transport in fine sandy loam soil under different flow rates. *Agricultural Water Management*, *83*, 111–118. https://doi.org/10.1016/j.agwat.2005.10.002

Dagan, G. (1986). Statistical theory of groundwater flow and transport: Pore to laboratory, laboratory to formation, and formation to regional scale. *Water Resources Research*, *22*(9), 120S-134S. https://doi.org/10.1029/WR022i09Sp0120S

De Smedt, F., Wauters, F., & Sevilla, J. (1986). Study of tracer movement through unsaturated sand. *Journal of Hydrology*, *85*, 169–181. https://doi.org/10.1016/0022-1694(86)90083-1

De Smet, F., Wierenga, P. J., & Beken, A. (1981). *Theoretical and experimental study of solute movement through porous media with mobile and immobile water*. *VUB Hydrologie (Belgium)*. VUB.

Devkota, L., Matsubayashi, U., & Takagi, F. (1998). A new form of dispersion coefficient model for the porous media. *Annual Journal of Hydraulic Engineering*, *42*, 355–360.

Fitch, A., & Jia, D. U. (1996). Solute transport in clay media: Effect of humic acid. *Environmental Science and Technology*, *30*(1), 12–15. https://doi.org/10.1021/es940133i

Gai, K., Shi, B., Yan, X., & Wang, D. (2011). Effect of dispersion on adsorption of atrazine by aqueous suspensions of fullerenes. *Environmental Science and Technology*, *45*(14), 5959–5965. https://doi.org/10.1021/es103595g

Geiger, S. L., & Durnford, D. S. (2000). Infiltration in homogeneous sands and a mechanistic model of unstable flow. *Soil Science Society of America Journal*, *64*(2), 460–469. https://doi.org/10.2136/sssaj2000.642460x

Gelhar, L. W. (1986). Stochastic subsurface hydrology from theory to applications. *Water Resources Research*, *22*(9), 135S-145S. https://doi.org/10.1029/WR022i09Sp0135S

van Genuchten, M. Th., & Wierenga, P. J. (1986). Solute dispersion coefficients and retardation factors. In *Methods of Soil Analysis, Part I: Physical and Minerological Methods. Agronomy Monograph No. 9* (pp. 1025–1053). American Society of Agronomy-Soil Science Society of America. https://doi.org/10.2136/sssabookser5.1.2ed.c44

van Genuchten, M. Th. (1980). A closed-form equation for predicting the hydraulic conductivity of unsaturated soils. *Soil Science Society of America Journal*, *44*, 892–898. https://doi.org/10.2136/sssaj1980.03615995004400050002x

van Genuchten, M Th., Wierenga, P. J., & O'Connor, G. A. (1977). Mass transfer studies in sorbing porous media: III. Experimental evaluation with 2,4,5-T. *Soil Science Society of America Journal*, *41*(2), 278–285. https://doi.org/10.2136/sssaj1977.03615995004100020023x

van Genuchten, M. Th., & Parker, J. C. (1984). Boundary Conditions for Displacement Experiments Through Short Laboratory Soil Columns. *Soil Science Society of America Journal*, *48*(4), 703–708. https://doi.org/10.2136/sssaj1984.03615995004800040002x

Karadimitriou, N. K., Joekar-Niasar, V., Babaei, M., & Shore, C. A. (2016). Critical role of the immobile zone in Non-Fickian two-phase transport: A New Paradigm. *Environmental Science and Technology*, *50*(8), 4384–4392. https://doi.org/10.1021/acs.est.5b05947

Kirda, C., Nielsen, D. R., & Biggar, J. W. (1973). Simultaneous Transport of Chloride and Water during Infiltration. *Soil Science Society of America Proceedings*, *37*(3), 339–345.

Kumahor, S. K., de Rooij, G. H., Schlüter, S., & Vogel, H.-J. (2015). Water flow and solute transport in unsaturated sand—A comprehensive experimental approach. *Vadose Zone Journal*, *14*(2). https://doi.org/10.2136/vzj2014.08.0105

Maraqa, M. A., Wallace, R. B., & Voice, T. C. (1997). Effects of degree of water saturation on dispersivity and immobile water in sandy soil columns. *Journal of Contaminant Hydrology*, *25*, 199–218. https://doi.org/10.1016/S0169-7722(96)00032-0

Matsubayashi, U., Devkota, L. P., & Takagi, F. (1997). Characteristics of the dispersion coefficient in miscible displacement through a glass beads medium. *Journal of Hydrology*, *192*, 51–64. https://doi.org/10.1016/S0022-1694(96)03120-4

Mayer, A., Sandman, T., & Breidenbach, M. (2008). Effect of flow regime on physical nonequilibrium transport in unsaturated porous media. *Vadose Zone Journal*, *7*(3), 981–991. https://doi.org/10.2136/vzj2007.0167

Padilla, I. Y., Yeh, T.-C. J., & Conklin, M. H. (1999). The effect of water content on solute transport in unsaturated porous media. *Water Resources Research*, *35*(11), 3303–3313. https://doi.org/10.1029/1999WR900171

Raoof, A., & Hassanizadeh, S. M. (2013). Saturation-dependent solute dispersivity in porous media: Pore-scale processes. *Water Resources Research*, *49*, 1943–1951. https://doi.org/10.1002/wrcr.20152

Rolle, M., Chiogna, G., Bauer, R., Griebler, C., & Grathwohl, P. (2010). Isotopic fractionation by transverse dispersion: Flow-through microcosms and reactive transport modeling study. *Environmental Science and Technology*, *44*(16), 6167–6173. https://doi.org/10.1021/es101179f

Scheidegger, A. E. (1961). General theory of dispersion in porous media. *Journal of Geophysical Research*, *66*(10), 3273–3278. https://doi.org/10.1029/JZ066i010p03273

Šimůnek, J., van Genuchten, M. Th., Sejna, M., Toride, N., & Leij, F. J. (1999). The STANMOD computer software for evaluating solute transport in porous media using analytical solutions of convection-dispersion equation. *IGWMC-TPS-71*. International Ground Water Modeling Center, Colorado School of Mines, Golden, CO.

Topp, G. C., Davis, J. L., & Annan, A. P. (1980). Electromagnetic determination of soil water content: Measruements in coaxial transmission lines. *Water Resources Research*, *16*(3), 574–582. https://doi.org/10.1029/WR016i003p00574

Toride, N., Leij, F. J., & van Genuchten, M. Th. (1995). The CXTFIT code for estimating transport parameters from laboratory or field tracer experiments. U.S. Salinity Laboratory Res. Rep. 137, U.S. Salinity, Riverside, CA.

Toride, N., Inoue, M., & Leij, F. J. (2003). Hydrodynamic dispersion in an unsaturated dune sand. *Soil Science Society of America Journal*, *67*, 703–712. https://doi.org/10.2136/sssaj2003.0703

Vanderborght, J., & Vereecken, H. (2007). Review of dispersivities for transport modeling in soils. *Vadose Zone Journal*, *6*, 29–52. https://doi.org/10.2136/vzj2006.0096

Yule, D. F., & Gardner, W. R. (1978). Longitudinal and transverse dispersion coefficients in unsaturated plainfield sand. *Water Resources Research*, *14*(4), 582–588. https://doi.org/10.1029/WR014i004p00582

Zhuang, L., Bezerra Coelho, C. R., Hassanizadeh, S. M., & van Genuchten, M. Th. (2017). Analysis of the hysteretic hydraulic properties of unsaturated soil. *Vadose Zone Journal*, *16*(5), 9p. https://doi.org/10.2136/vzj2016.11.0115